INTERNATIONAL JOURNAL FOR NUMERICAL METHODS IN FLUIDS
Int. J. Numer. Meth. Fluids 2007; **54**:1119–1130
Published online 23 January 2007 in Wiley InterScience (www.interscience.wiley.com). DOI: 10.1002/fld.1422

Modelling of the free surface with heat and mass transfer considerations on a liquid filling a porous slab heated from its sides

S. M. Prabhu[1,*,†] and T. Soundarajankrishnan[2]

[1]*Department of Chemical Engineering, Shanmuga University, Thanjavur, Tamil Nadu, India 613 402*
[2]*Chemical Engineering, Satyabama Deemed University, Chennai, Tamil Nadu, India*

SUMMARY

The position of the free surface is calculated numerically for a porous slab which is partly filled with a liquid and differentially heated from its sides. A coordinate transformation is used to transform the original problem from a physical coordinate system to a non-orthogonal system where the free surface becomes a fixed straightline. The transformed problem is then solved using a finite difference method. Results are obtained for Rayleigh numbers up to 1000. The Nusselt numbers increase slightly with medium Rayleigh numbers (convection-dominated region) as expected. Since at low *Ra* the conduction is dominant and at high *Ra* radiation is dominant. Hadizadeh and Tien (*Int. J. Heat Mass Transfer* 2004; **17**(6):799–804) studied the forced convection on the surface of porous layer. In that paper they dealt with in detail the boundary regime of liquid in the channel and modelled the flow and heat transfer. Copyright © 2007 John Wiley & Sons, Ltd.

Received 14 June 2006; Revised 3 October 2006; Accepted 31 October 2006

KEY WORDS: surface region; porous channel; finite difference method; coordinate transformation method; coupled heat and mass transfer

INTRODUCTION

The study of porous media in which liquid saturation and thermal diffusion take place are currently of high interest in many fields. The diffusion of oil and gas in oil wells, leaching of ores and steam generation using porous enclosures requiring fast heat disposal are some of the applications in which the liquid filling a porous slab is used. The steady fully saturated flow in a porous medium with heat conduction is considered for the case where the upper boundary consists

*Correspondence to: S. M. Prabhu, Department of Chemical Engineering, Shanmuga University, Thanjavur, Tamil Nadu, India 613 402.
†E-mail: prabhusm2005@yahoo.co.in

of a free surface. The model consists of Poisson equation for the stream function, the steady diffusion convection equation for the temperature and a first-order equation for the free surface together with appropriate boundary conditions. In the study by Rasmussen [1] this problem was dealt with by a analytical solution using a small Rayleigh number perturbration for the case of porous slab partly filled and differentially heated from the sides. A first-order expression for the free surface and a third-order approximation to the heat transfer across the slab were obtained from an asymptotic solution. There are two main difficulties numerically. First, the mathematical model is nonlinear since both the diffusion equation and the free surface equation are coupled by two nonlinear terms. Hence, they have to be converted to discrete form like difference equations and solved by iteration. The second difficulty is the irregular-shaped domain with the free surface which makes it difficult to apply finite difference methods directly. In this we use coordinate transformation which transforms the original domain into a rectangular domain where the finite differences can be obtained. The resulting model was solved for different values of the Rayleigh number *Ra*, and we present numerical results for the free surface and the heat transfer.

The porous slabs are used in combined lubrication and thermal insulation to rotating machines like turbines, fans, compressor and motor shafts and in systems where heat dissipation is of high importance. They are used for providing indirect heat in vacuum distillers, chemical reactors with indirect and controlled heating bioreactors, vacuum and steam-heated tube dryers where steam, oil or a thermic fluid is used to provide heat. The heat is supplied using hot vapour, steam or a thermic fluid in by slowly perfusing through a porous enclosure. They are also used as coolant circuits in nuclear reactors and in thermofusion reactors as diverters.

Many papers which deal with either diffusion convection or free surface exist [2–6], but a combined solution was not dealt with earlier. Loh and Rasmussen [7] studied the free surface convection while Hadizadeh and Tien [2] studied the forced convection on the surface of the porous layer. In that paper they dealt with in detail the boundary regime of liquid in the channel and modelled the flow and heat transfer. In this paper, we compare our data with that of Hadizadeh and Tien [2] for the Nusselt and Rayleigh numbers. Lai [3] discussed the adiabatic convection for a line heat source. Pop and Postelneicu [4] discussed the effect of heat generation on the layers in porous media. Ras and Pop [5] reported the free convection in a concrete slab due to water seepage and corresponding heat effects. Ras [6] delved on the models for natural convection in porous media with stagnation point flow. Yin [8] studied the forced convection in porous media. Pop [9] studied the surface fluid layer and the energy analysis of the surface layer. Rasmussen [10] studied the effect of non-Darcy convection in the free surface of a porous media. But the previous workers did not deal with the combined hydrodynamics and heat transfer for accounting the shape of the liquid in the porous slab (porous regime).

In this paper, a generalized treatment for convection force and the effect of free surface hydrodynamics on the heat transfer are dealt with. A novel model incorporating computation of local and average heat flux has been discussed. The effect of the depth of the surface and geometry of the porous media are modelled. A coordinate transformation technique has been used to take relative magnitudes of the velocity and temperature gradients. A finite difference technique which is simple and convenient has been used to solve the model. Rayleigh number, Nusselt number and Darcy number have been computed. All the results are compared with Hadizadeh and Tien [2], Rasmussen [1, 9] and other literature in the field.

DOI: 10.1002/fld

EXPERIMENTAL METHODS

A porous aluminium insert is placed in a small square recess made on a curved (5 cm × 5 cm) metal plate. The metal plate is kept horizontally in a rectangular tank with. Copper-constantan/K-type thermocouples. A cooling device with temperature measurement and control is connected to the tank and castor oil is heated to 5°C. The curved plate is wound with a nichrome heating wire and connected to a voltage source. Since the metal plate is curved there is a varying heat flux along the surface of the curved plate. The coolant (castor oil is heated as it flows along the plate) is allowed to flow into the rectangular tank. It penetrates the porous insert and comes out.

The distribution of the coolant is controlled so that the surface has uniform heat flux. This is done by varying the depth of immersion of metal plate in the coolant by keeping it sloping at a angle of 10–12° as shown in Figure 1(a).

Mathematical model

The two-dimensional (2D) porous region is shown in Figure 1(a). The curved upper and lower boundaries are permeable, while the side boundaries are joined to a solid wall and hence have no flow through them. The upper reservoir contains coolant at P_∞, L_∞, which is pumped into the region. The coolant is pumped into the upper reservoir region through the boundary s. The coolant flows out through s_0 which is at uniform pressure p_0 and has a heat flux $q_0(x, y)$ imposed along it. The coolant flow distribution through s_0 is to be regulated, to carry away the heat load and maintain the surface s_0 at a specified temperature t_0. This is accomplished by having a proper shape of the

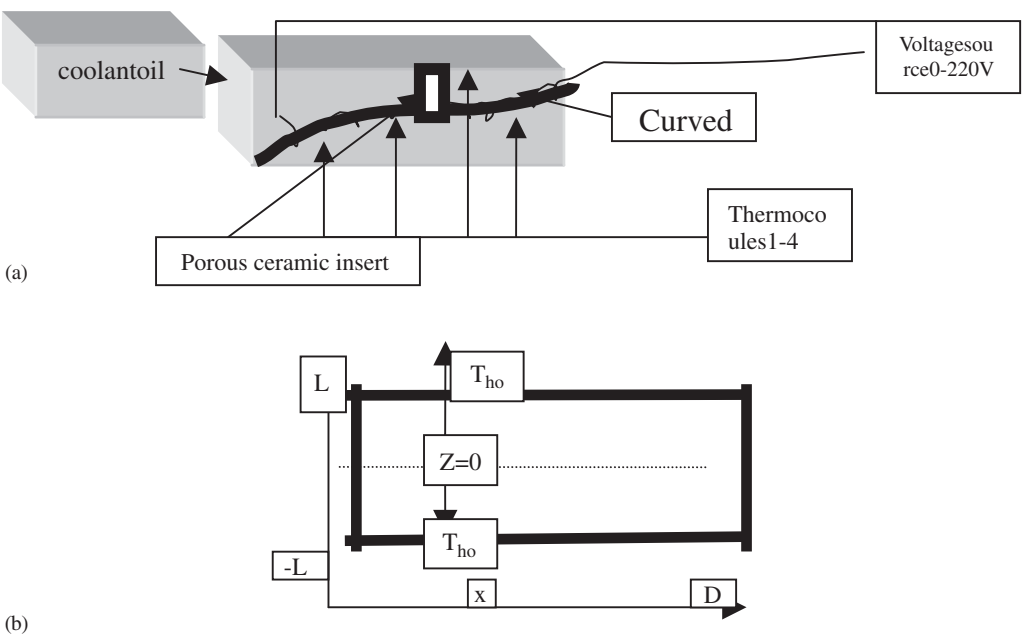

Figure 1. (a) Experimental set-up for the heat flux studies in a porous insert; and (b) flow configuration.

DOI: 10.1002/fld

upper curved surface. The correct region shape will provide the required flow distribution and heat conduction within the porous structure such that s_0 will be at the desired uniform temperature. In many instances, the flow resistance of the porous medium is large enough such that $p_\infty - p_0$ is much greater than any pressure variations along the porous boundaries. Hence, they are assumed to be uniform.

Formulation

The flow configuration of the porous slab is given in Figure 1(b). We consider a long porous slab of width D which is partly filled with a liquid. At the reference temperature T_0 the liquid occupies the region $0 \leqslant x \leqslant D$, $-L \leqslant z < 0$; the line $z = 0$ is the free surface of the liquid. In general, we represent this by $z = h(x)$ where $h(x)$ is the unknown function of x.

The flow field is given by the continuity equation

$$\nabla \cdot (\rho \mathbf{v}) = 0$$

and Darcy's law

$$\rho \mathbf{v} = -K(\nabla P + \rho g k) \tag{1a}$$

where k is the unit vector in the positive z direction. The temperature field is given by heat conduction equation

$$c\rho\, \mathbf{v} \cdot \nabla T = \lambda \nabla^2 T \tag{1b}$$

where c is the specific heat, T temperature and λ the coefficient of thermal conductivity. We also require an equation of state which gives the dependence of density on temperature. For most liquids, it is adequate to suppose that this relationship is linear; thus, we use

$$\rho = \rho_0[1 - \beta(T - T_0)]$$

β is the volumetric thermal expansion coefficient and ρ_0 and T_0 are the reference values.

At the free surface and at the bottom of the slab the heat flow is set to zero, while the two sides are kept at different temperatures

$$\left.\begin{aligned} \frac{\partial T}{\partial z} = 0, \quad v_z = 0 \quad &\text{at } z = -L \\ T = T_0 - \tfrac{1}{2}\Delta T, \quad v_x = 0 \quad &\text{at } x = 0 \\ T = T_0 + \tfrac{1}{2}\Delta T, \quad v_x = 0 \quad &\text{at } x = D \end{aligned}\right\} \tag{1c}$$

$$\left.\begin{aligned} \frac{\partial T}{\partial z} - h' \frac{\partial T}{\partial x} = 0 \\ v_z - h' v_x = 0 \\ P = 0 \end{aligned}\right\} \quad \text{at } z = h(x) \tag{1d}$$

The first boundary condition on the free surface $z = h(x)$ states that the normal temperature gradient is zero corresponding to zero heatflux; the second condition is the kinematic boundary condition which expresses the fact that fluid particles which are the free surface initially remain

DOI: 10.1002/fld

there. We assume that the pressure at $z=h(x)$ is constant and since only ΔP appears we can take this constant to be zero, this gives the third condition. It should be noted that for the concept of a sharp interface between a fully saturated and completely unsaturated zone, the mathematical model presented above may not be valid. But in most of the practical situations the depth of this intermediate zone will be small compared to the other characteristic lengths of the problems such as the width of the slab. The results of the present model give a reliable solution for the complete problem.

We define the non-dimensional variables by

$$X^*=\frac{x}{D},\quad z^*=\frac{z}{D},\quad \nabla^*=D\nabla$$

$$h^*(x^*)=\frac{h(x)}{D}$$

$$\mathbf{u}=\frac{v}{K\rho g\beta\Delta T}\rho\mathbf{v}$$

$$\theta=\frac{T-T_0}{\Delta T}$$

And a non-dimensional potential by

$$\phi=\left(\frac{P}{\rho_0 g}+z\right)\frac{1}{D\beta\Delta T} \tag{2}$$

In the following non-dimensional formulation, we denote x^*, z^* and h^* by x, z, h for convenience. If we define a stream function Ψ such that

$$u_x=\Psi_z \quad \text{and} \quad u_z=-\Psi_x$$

the governing equations can be written in the form

$$\nabla^2\Psi=-\theta_x \tag{2a}$$

$$\nabla^2\theta=Ra(\Psi_z\theta_x-\Psi_x\theta_z) \tag{2b}$$

where the Rayleigh number is given by

$$Ra=\frac{cK\rho gD\varepsilon}{\Lambda v}$$

and $\varepsilon=\beta\Delta T$.

The corresponding boundary conditions of (1d) become

$$\left.\begin{aligned} \text{at } x=0,\quad & \theta=-\tfrac{1}{2},\quad \Psi=0 \\ x=0,\quad & \theta=-\tfrac{1}{2},\quad \Psi=0 \\ z=-L/D=-\gamma,\quad & \theta_z=0,\quad \Psi=0 \end{aligned}\right\} \tag{2c}$$

DOI: 10.1002/fld

Numerical procedure

Since we wish to apply finite difference method, it is convenient to use a coordinate transformation method to transform irregularly shaped domain $0<x<1$, $-r<z<h(x)$ into a regularly shaped domain where all boundaries will coincide with the grid lines. Hence, we let $x_0 = z = 0$.

The non-uniform mesh was used since it is known that most of the variation in ψ and θ takes place near the boundaries. Hence, a non-uniform mesh with lines concentrated in these regions will give the best accuracy. Standard difference approximations are used and the changes in mesh openings are smooth enough so that second-order accuracy is obtained throughout the region. The numerical procedure for solving the boundary value problems (6)–(14) consists of two parts: in the first part, the field Equations (6) and (7) together with the boundary conditions (8)–(10) are solved for θ and ψ given the free surface function $h(x)$; while in the second part Equations (13) and (14) are solved for $h(x)$ given ψ and θ. Since these two parts are coupled, it is necessary to use an iterative procedure. Thus, if h_i^n is the nth approximation to $h(x)$ given ψ and θ; these values are then used in Equations (13) and (14) which is solved for h_i^{n+1}. This iterative procedure is continued until $\max |h_i^{n+1} - h_i^n| < 10^{-5}$.

With given $h_i^n \theta^{n+1}$, $\psi_{i,j}^{n+1}$ is as follows. We use the second-order difference formulae to replace Equations (6) and (7) by corresponding difference equations; upwind downwind formulae were not used. Since these algebraic equations are nonlinear, an iterative procedure must be used. The RHS of Equation (6) is evaluated using h_i^{n+1} and θ_i^{n+1}, and the resulting net of algebraic equations for an approximation to ψ_{ij} are swept once again using a line SOR (sum of residues). The values are then used in equations to evaluate θ_i and ψ_i in Equation (7) until the difference between the two consecutive iterates is less than the given tolerance. These are then solved for h_i^{n+1}

$$\text{At } z = h(x) \begin{cases} -\Psi_z + h(\Psi_x + \theta) = \dfrac{h'}{\varepsilon} \\ \theta_z - h'\theta_z = 0 \\ \psi = 0 \end{cases} \tag{3}$$

since the mass is conserved we can write another relation (in non-dimensional form) as below

$$\int_0^1 h \, \mathrm{d}x = \int_0^1 \int_{-\gamma}^{h} \beta \Delta T \, \theta \, \mathrm{d}z \, \mathrm{d}x \tag{4}$$

Now, we analyse how the free surface affects the heat flux in the porous slab. At $x = 0$ the heat flux in the slab is given by

$$q = \theta(0, z) \, \mathrm{d}z \tag{5}$$

Here, the integral is computed along the sidewall $x = 0$ which forms an isotherm.

Now we convert the coordinate to transform the irregular domain $0 \leqslant x \leqslant 1$, $-\gamma \leqslant z \leqslant h(x)$ to the regularly shaped domain where all boundaries will coincide with grid lines.

This is needed for a numerical solution of the above model using a finite difference method. Hence, in (3)–(5) we let

$$x = 0, \quad y = \frac{z - h(x)}{h(x) + \gamma} \gamma$$

DOI: 10.1002/fld

Hence, we get the transformed variables as

$$\text{At } z = -\gamma \rightarrow y = -\gamma$$

and

$$\text{at } z = h(x) \rightarrow y = 0$$

In terms of the new coordinates, Equations (1)–(2) become

$$D^2\psi = -\theta_x + h\frac{z+\gamma}{h+\gamma}\theta_y \tag{6}$$

$$D^2\theta - Ra\frac{\gamma}{h+\gamma}[\psi_y\theta_x - \theta_y\psi_x] = 0 \tag{7}$$

where

$$D^2 = \frac{\partial^2}{\partial x^2} - \frac{2h'}{(h+\gamma)}\frac{\partial^2}{\partial x\partial y}\frac{h'^2(z+\gamma)^2+\gamma^2}{(h+\gamma)^2}\frac{\partial^2}{\partial y^2} + \frac{(y+\gamma)}{(h+\gamma)^2}[2h'^2 - (h+\gamma)]\frac{\partial}{\partial y}$$

and

$$\theta = -\tfrac{1}{2}, \quad \psi = 0 \quad \text{at } x = 0 \tag{8}$$

$$\theta = \tfrac{1}{2}, \quad \psi = 0 \quad \text{at } x = 1 \tag{9}$$

$$\theta_z = 0, \quad \psi = 0 \quad \text{at } y = -\gamma \tag{10}$$

$$\psi = \psi_y \quad \text{at } y = 0 \tag{11}$$

$$\theta_z - \frac{h'(h+\gamma)}{\gamma(1+h^2)}\theta_x = 0 \quad \text{at } y = 0 \tag{12}$$

$$h' = -\frac{\gamma\psi_y}{[(1/\varepsilon) - \theta](h+\gamma) - \gamma h'\psi_y} \quad \text{at } y = 0 \tag{13}$$

Here we have replaced x_0 by x for generalizing. The mass conservation Equation (4) and the heat transport Equation (5) become

$$q = \frac{\lambda\Delta T}{\gamma}\int_{-\gamma}^{0}(h+\gamma)\theta_x(0, y)\,\mathrm{d}y \tag{14}$$

The region $0 \leqslant x < 1$, $-\gamma \leqslant y \leqslant 0$ is covered with a non-uniform finite difference mesh defined by

$$\left.\begin{aligned} 0 = x_1 < x_2 < \cdots < x_{N+1} = 1 \\ \text{and } -\gamma = y_1 < y_2 \cdots < y_{M+1} = 0 \end{aligned}\right\} \tag{15}$$

Now we use the notation $\psi_{i,j} = \psi(x_i, y_j)$.

DOI: 10.1002/fld

Table I. Local heat flux $h(x)$ for different values of Ra with $\varepsilon = 0$, $\gamma = 1.0$.

Ra	$z=0$ (results of [2])	$z=0$	$z=1$	$z=0.2$	$z=0.4$	$z=0.6$	$z=0.8$	$z=1$ (results from [2])
Local heat flux $h(x)$								
0.1	−0.125	−0.12	0.123	−0.09	−0.03	0.033	0.093	0.125
100	−0.04	−0.033	0.0533	−0.011	0.0091	0.029	0.041	0.0509
300	−0.03	−0.028	0.041	−0.05	0.011	0.025	0.0364	0.044
500	−0.023	−0.021	0.03	−0.002	0.011	0.022	0.033	0.038
800	−0.0171	−0.05	0.029	0.00	0.011	0.02	0.028	0.034
1000	−0.016	−0.006	0.0328	0.001	0.011	0.0189	0.026	0.032

Table II. Values of Nusselt numbers with $\varepsilon = 0.35$, $\gamma = 1$.

Ra	Nu (experimental)	Nu (numerical solution)	Nu (from [2])
100	2.3	>2.2	1.9
250	5.44	<5.32	5.4
350	8.33	>8.31	8.6
500	11.3	>11.34	11.3
800	13.4	>13.34	13.6
1000	15.67	>15.7	15.8

A second-order difference approximation to Equation (13) is

$$h_i + 1 = -[(\gamma/2\Delta)(\psi^{n+1}_{\text{im}\,M-1} - 4\psi^{n+1}_{I,M})]/\{[(1/\varepsilon) - (\gamma^{n+1}_{I,M})] \times x(h^{n+1}_i + \theta) - (\gamma/2\Delta)h^n_i(\psi^{n+1}_{I,M})\} \tag{16}$$

where $h_1 = h'_1$ and we have assumed the two grid spacings next to $z = 0$ are equal so that

$$\Delta = z_{M+1} - z_M = z_M - z_{M-1}$$

Hence, we have

$$h^{n+1}_i = \int h^{n+1}_i \,\mathrm{d}x + \varepsilon \int_0^1 \int_{-\gamma}^0 (h^{n+1} + \gamma)\theta^{n+1} \,\mathrm{d}z)\,\mathrm{d}x - \int_0^1 \int_0^x (h^{n+1}\,\mathrm{d}\sigma)\,\mathrm{d}x \tag{17}$$

Equations (16) and (17) are coupled nonlinear forms of h^{n+1}_i when ψ^{n+1}_I and θ^{n+1}_I are given. They were solved by direct iteration with integrals in Equations (14) and evaluated using trapezoidal rule. The convergence was accelerated by using over relaxation of the variable. The final heat flux q can be calculated by a numerical computation of (14).

Numerical solution for the case where the top surface is not free but fixed with a lid at $z = 0$ is also shown in Tables I and II.

For the boundary conditions of a fixed lid we have

$$\theta_z = 0, \quad \psi = 0 \quad \text{at } z = 0$$

Here the outer iteration is not required as done for the free surface as it is a closed lid.

DOI: 10.1002/fld

RESULTS AND DISCUSSION

The plots of *Ra vs* the local heat flux $h(x)$ are shown in Figure 3 for $z=0.4$ and 0.4. Figure 2 shows the plot of Rayleigh number with local heat flux at $z=0.2$. The heat flux plot of Figure 7 shows these values at $z=0.8$. As we see the values of $h(x)$ increase continuously along the distance z for same Rayleigh numbers, and for the same value of z they increase slightly. Only for $z=0$ the $h(x)$ values are negative, they have an increasing tendency to positive value at $z=0.2$ and subsequently become higher along the distance. This may be attributed to the fact that conduction and radiation-dominated flow at the far end of the channel is high (i.e. at higher Rayleigh numbers) since the inlet velocity is less. Heat dissipation occurs away from the hot end and continuously decreases as the distance (axial) increases. Figure 4 shows the Rayleigh number *vs* heat flux for $z=0.6$.

Figure 5 shows the plot of Nusselt numbers (experimental) and Figure 6 Nusselt numbers (computed by model) for various Rayleigh numbers. Both are in close agreement except at low *Ra* (convection-dominated flow). The Nusselt numbers increase slightly with medium Rayleigh numbers (convection-dominated region) as expected. Since at low *Ra*, the conduction is dominant

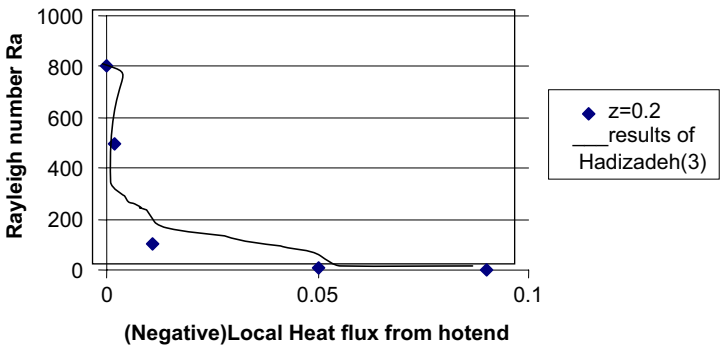

Figure 2. Rayleigh number for $z=0.2$ with heat flux $h(x)$.

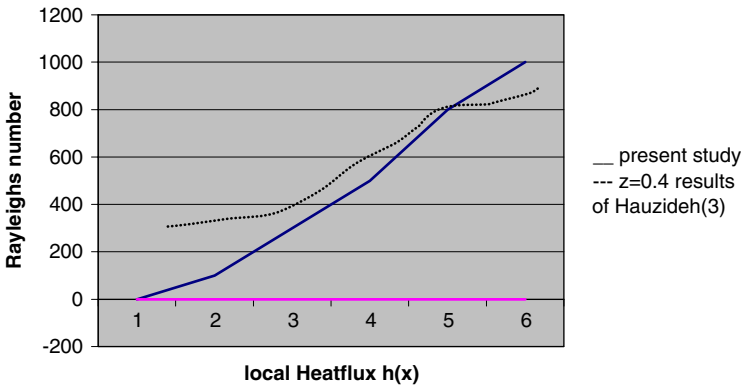

Figure 3. Plot of *Ra vs* heat flux $h(x)$.

DOI: 10.1002/fld

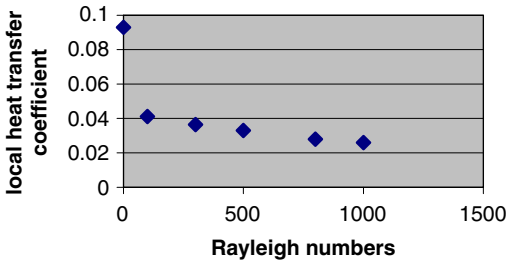

Figure 4. Plot of Rayleigh number *vs* heat transfer coefficient, $h(x)$ for $z = 0.6$, $\gamma = 1$.

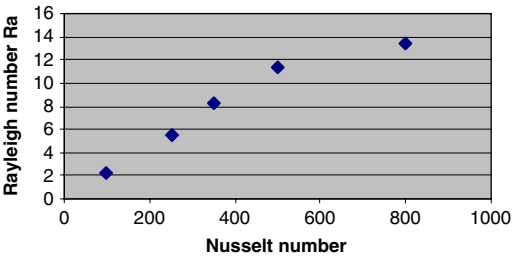

Figure 5. Plot of *Ra vs Nu* (experimental, series 2-results of Hadizadeh and Tien [2]).

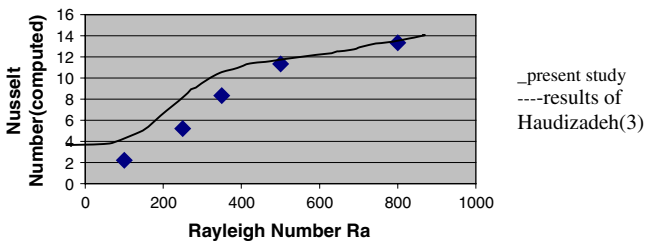

Figure 6. Plot of *Ra vs* Nusselt number (numerical solution).

and at high *Ra*, radiation is dominant. These results are in agreement with those of Hadizadeh and Tien [2] as shown in Figures 3, 4 and 7 for local heat flux and in Figure 6 for Nusselt numbers. These results point out in general, that high Rayleigh number causes high convection, i.e. at lower *Ra* of 1 and below radiation is dominant and convection practically absent hence the negative and increasing heat flux even at a considerable distance from the hot end. And as Rayleigh number crosses $Ra = 10$ and increases to $Ra = 100$ convection is equally influencing between $Ra = 1$ and 10 though not dominant.

DOI: 10.1002/fld

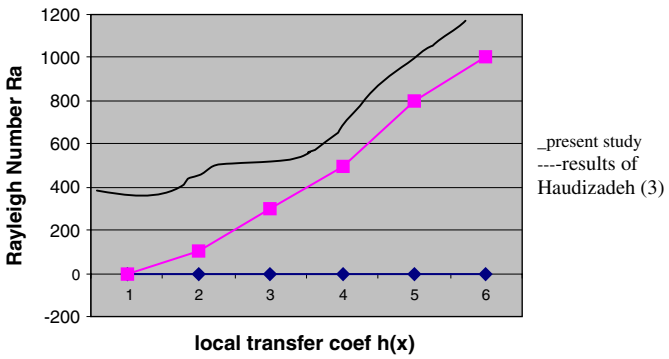

Figure 7. $h(x)$ *vs* Ra at $z = 0.1$ series 12 (results of [2]).

CONCLUSIONS AND SUGGESTIONS

The porous slabs are used for providing indirect heat in vacuum distillers, chemical reactors with indirect and controlled heating bioreactors, vacuum and steam-heated tube dryers where steam, oil or a thermic fluid is used to provide heat. The heat is supplied using hot vapour, steam or a thermic fluid in by slowly perfusing through a porous enclosure. They are also used in coolant circuits in nuclear reactors and in thermofusion reactors as diverters.

The coordinates of the surface region is converted to transform the irregular domain $0 \leqslant x \leqslant 1$, $-\gamma \leqslant z \leqslant h(x)$ to the regular-shaped domain where all boundaries will coincide with grid lines. This was needed for a numerical solution of the above model using a finite difference method.

For the case of no through flow, buoyancy-driven flow is the only mode of convective motions. Since the effect of through flow on this basic flow structure is under consideration. All calculations for this case were performed for values of R ranging up to 80 and four different aspect ratios $L = 2, 3, 4, 5$. The Nusselt numbers increase slightly with medium Rayleigh numbers (convection-dominated region) as expected. Since at low Ra, the conduction is dominant and at high Ra, radiation is dominant. Hadizadeh and Tien [2] studied the forced convection on the surface of porous layer. In that paper they dealt with in detail the boundary regime of the liquid in the channel and modelled the flow and heat transfer. Also, we compare our data with those of Hadizadeh and Tien [2] for the Nusselt and Rayleigh numbers. These results are in agreement with the reported results.

NOMENCLATURE

A	shape parameter of the curved heated surface
B	amplitude
D	diffusion parameter
H	amplitude f variation in heat input
K_{m}	thermal conductivity of porous media
$M = (\mu/2\mu_\infty)(t_\infty/t)$	for incompressible flow
φ, ψ_{m}	(= maximum value of ψ)
	(μ/μ_∞) for compressible flow
n	coordinate in the direction of outward normal N_{w}

DOI: 10.1002/fld

P	for incompressible flow (p/p_∞); for compressible flow $(p/p_\infty)^2$ entrance surface
p	pressure bar, q-heatflux ((w/m^2) boundary)coolant exit surface
s	distance curved boundary S_w
Temperature ratio	(t/t_∞)
t	absolute temperature K
$\mathbf{u}$	coolant velocity vector
w	width of porous region along the x-axis
X, Y	Cartesian coordinates x/w, y/w
X_0, Y_0	functions $X(\psi)$, $Y(\psi)$ along S_0
x, y	Cartesian coordinates
Z	complex variable $X + iY$
K	permeability

Greek symbols

η	pore diameter function $(= \pi\varphi_s/\psi)$
μ, ρ	coolant viscosity and density
φ	potential function
v	kinematic viscosity
ψ	function orthogonal to
∇^2	$\partial^2/\partial X^2 + \partial/\partial Y^2$ (Kronecker delta function)

Subscripts

s	point at shaped coolant
0	point at curved
∞	conditions in coolant tank

REFERENCES

1. Rasmussen H. Analytical solution using a asymptotic method. *International Journal of Heat and Mass Transfer* 1981; **13**(12):191–194.
2. Hadizadeh M, Tien CL. Natural and forced convection in a porous channel. *International Journal of Heat and Mass Transfer* 2004; **17**(6):799–804.
3. Lai FC. NonDarcy convection from a line source. *International Communications in Heat and Mass Transfer* 1994; **12**(17):875–880.
4. Postelneicu A, Pop I. Convection in porous media with generation. *International Journal for Numerical Methods in Heat Transfer* 2002; **26**(8).
5. Ras DAS, Pop I. Modeling of natural convection in shallow porous concrete slab to control heatflow. *International Communications in Heat and Mass Transfer* 1999; **26**(6):761–770.
6. Ras DAS. Free convection stagnation point flow in a porous media in a thermal nonequilibrium region. *International Communications in Heat and Mass Transfer* 1990; **12**:162–171.
7. Loh CY, Rasmussen H. The free surface convection on a liquid filling a porous slab heated from its sides. *International Journal of Heat and Mass Transfer* 1984; **27**(6):921–926.
8. Yin KA. Mixed convection of fluid in a porous and concentration distribution in the entire regime. *International Communications in Heat and Mass Transfer* 1999; **26**(7):1041–1050.
9. Pop I. Analysis of free surface momentum and energy transport in porous media. *Numerical Heat Transfer*, *Part A* 1996; **29**:281–296.
10. Rasmussen H. Non Darcy surface effect on the free surface from a porous model. *Numerical Heat Transfer Journal*, *Part A* 1997; **31**:235–254.

DOI: 10.1002/fld